ISOSTASY AND CRUSTAL STRUCTURE IN THE ENGLISH RIVER GNEISSIC BELT

A Thesis

Presented to

The Faculty of Graduate Studies and Research

University of Manitoba

In Partial Fulfillment

of the Requirements for the Degree

Master of Science, Geophysics

---

by

Robert James Brown

August, 1968

ABSTRACT

Seismic studies carried out by the Department of Geology, Mineralogy and Geophysics, the University of Manitoba, have revealed an east-west trending structural feature in the crust below the English River gneissic belt, characterized by a thickened upper crustal layer, a thinned lower crustal layer and high or bulge in the mantle.

Three crustal models are considered: first, a continuous crust with warps in the Intermediate and Mohorovicic discontinuities and with uniform density in each layer; secondly, a crust of stratified blocks with vertical sides; and thirdly, a parallelepiped block model with allowance for density variation in the upper crustal layer.

The crust throughout the study area appears very close to being in local isostatic equilibrium. Isostatic and gravity comparisons suggest a greater average density below the gneissic belt of a few hundredths of a gm./cm.^{3} throughout several kilometers depth of the crust. It seems most likely that this density anomaly lies in the upper crustal layer and nearer its top. Including the effect of this mass, the south and central blocks of the crustal model appear to be in isostatic equilibrium. The north block appears to be slightly deficient in mass in comparison with the other two.

ACKNOWLEDGEMENTS

I would like to thank Dr. D. H. Hall of the Department of Geology, Mineralogy and Geophysics, the University of Manitoba for his abundant assistance throughout the preparation of this thesis. Prof. W. C. Brisbin and Dr. H. D. B. Wilson of the Geology Department and Dr. H. R. Coish of the Department of Physics provided valuable discussion and suggestions for which I am grateful. Dr. Hall, Mr. Z. Hajnal and Prof. Brisbin have kindly allowed me free use of their geophysical data for which I am most appreciative. Figures 2, 3 and 4 have been reproduced from Hall and Hajnal (1968) with their permission.

The financial support which made this study possible was provided in 1966-67 through a grant-in-aid of research from the Geological Survey of Canada and the University of Manitoba Northern Studies Committee, and in 1967-68 by a graduate fellowship from Northern Electric Company Limited.

TABLE OF CONTENTS

LIST OF ILLUSTRATIONS

CHAPTER I

INTRODUCTION

Purpose of the Study

The purpose of this study is to take the seismic data in the form of interface depths and velocities and using accepted velocity-density relations attempt to determine the isostatic state of the crust underlying the English River gneissic belt. In addition, any inadequacies in the seismic crustal model to explain observed gravity anomalies are examined with a view to producing an improved crustal model. Possible origins of the crustal structure are considered briefly as well.

Geographical Location

The area of this study is located in northwestern Ontario and adjacent eastern Manitoba. It extends approximately from Lake Winnipeg in the west to Lac Seul in the east, and from McCusker Lake in the north to Lake of the Woods in the south (Figure 1). It is bounded roughly by longitudes $92^{o}30'$ and $96^{o}00'$, and by latitudes $49^{o}30'$ and $51^{o}45'$, and covers an area of some 20,000 square miles. The English-Winnipeg River system flows through the area connecting Lac Seul and Lake of the Woods in the east and south respectively, with Lake Winnipeg in the west. The towns of Kenora, Ontario, in the south, Red Lake, Ontario, in the northeast and Bissett, Manitoba, in the northwest are included in the area.

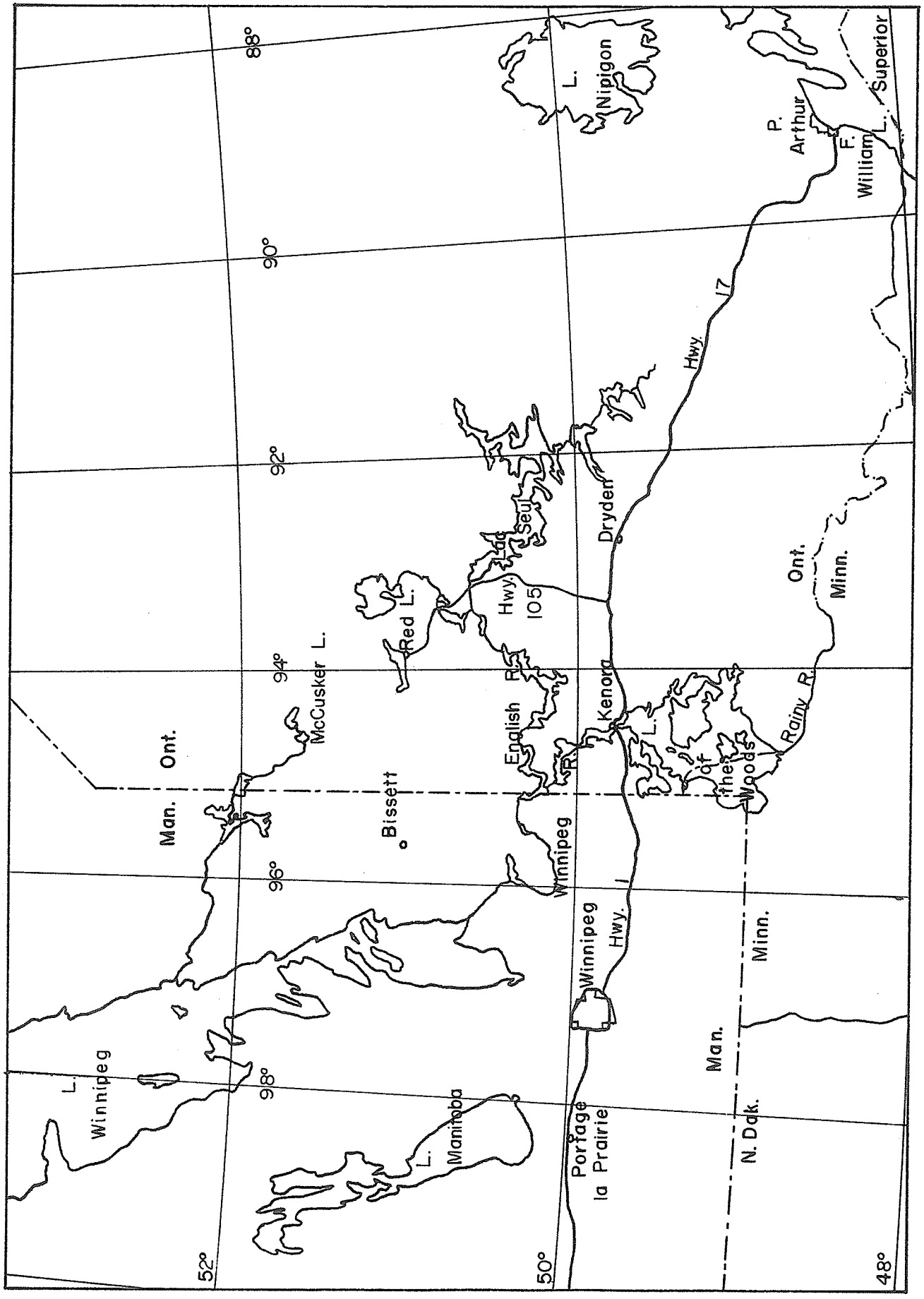

FIGURE 1. LOCATION MAP

CHAPTER II

OBSERVATIONS AND INFORMATION AVAILABLE

Geology

The entire study area lies within the Superior province of the Canadian Shield. In the southern part of the Superior province, which includes the study area, linear belts appear to be aligned in east-west trending patterns (Goodwin, 1968). The English River gneissic belt, about 80 to 100 km. in width runs through the study area. It is a zone of high-grade metamorphic rocks believed to be, at least in part, paragneisses (Dwibedi, 1966). North and south of the gneissic belt are complex belts consisting of volcanic-sedimentary assemblages known as greenstones separated by diapiric granitic plutons. The greenstones and gneisses are both of Archaean age. The volcanic assemblages show evidence of subaqueous accumulation and explosive derivation suggestive of continental environments including island arcs (Goodwin, 1968).

The gneissic belt is remarkably free of the greenstone so common to the south and north. In the complex belts of volcanic and sedimentary rocks, and granitic plutons, the greenstones seem to run in northeast and northwest trending belts enclosing the granitic bodies (Wilson and Brisbin, 1968).

Striking east-west trending lineaments have been mapped in the study area from aerial photograph compilation (Parkinson, 1962) and from aerial photographs together with magnetic anomaly maps (Wilson and Brisbin, 1968). The most pronounced of these lineaments appear to lie along the borders of the English River gneissic belt. These have been interpreted by Wilson and Brisbin (1968) as possible faults bounding the gneissic belt. These lineaments trend east-west from Lake Winnipeg, about 96^{o} longitude, to Lake Nipigon, about 89^{o} longitude, where a structural change occurs.

Elevations throughout the area are essentially constant. Topographic variations are of short wave-length so that no heights or depressions are of sufficient horizontal extent to enter into isostatic compensation. The maximum topographic relief is roughly 100 m. from an average elevation of about 350 m. above sea level.

Goodwin (1968) and Wilson (1949) have discussed a theory of continental growth whereby protocontinents grew separately by the addition of marginal orogenic belts around nuclei, or cratons, which formed very early in the Earth's history. Several such protocontinents corresponding to the geological provinces of the Canadian Shield are thought to have grown together and merged. According to Goodwin one craton lies in northwestern Ontario and adjacent Manitoba, north of the study area. The complex belt just north of the English River gneissic belt lies along the southern margin of this granitic metasedimentary craton.

This theory, while it may provide a partial explanation of the origin of the gneissic belt, is still unproved. Submission of conclusive evidence for or against any particular origin is beyond the scope of this thesis. It is hoped that some small contribution to the large problem will, however, result.

Seismic Information

A detailed refraction seismic survey of the study area has been carried out by the seismic group of the Department of Geology, Mineralogy and Geophysics of the University of Manitoba, and has been reported by them (Hall and Hajnal, 1968). The coverage of their survey is continually being extended westward and northward. Figure 2 is a reproduction of their Figure 1 (Hall and Hajnal, 1968), showing the shot and recording sites. Their interpretation indicates a two-layer crustal model. They refer to the interface between the two crustal layers as the Intermediate discontinuity and suggest it might be the same as the Conrad discontinuity of European seismologists, or the Riel discontinuity of Alberta (Clowes, Kanasewich and Cumming, 1968).

Figures 3 and 4 are reproductions of Figures 8 and 9 of Hall and Hajnal (1968) showing depths as interpreted by them and the resulting contour maps of the Intermediate and Mohorovicic discontinuities. Their calculation of depths was done by a method resembling that of Gardner (1939) using delay times and offsets. This method of interpretation gives depths more accurately than the standard time-term method which leads to considerable averaging, tending to obscure rapid changes in interface depths (Hall, 1968).

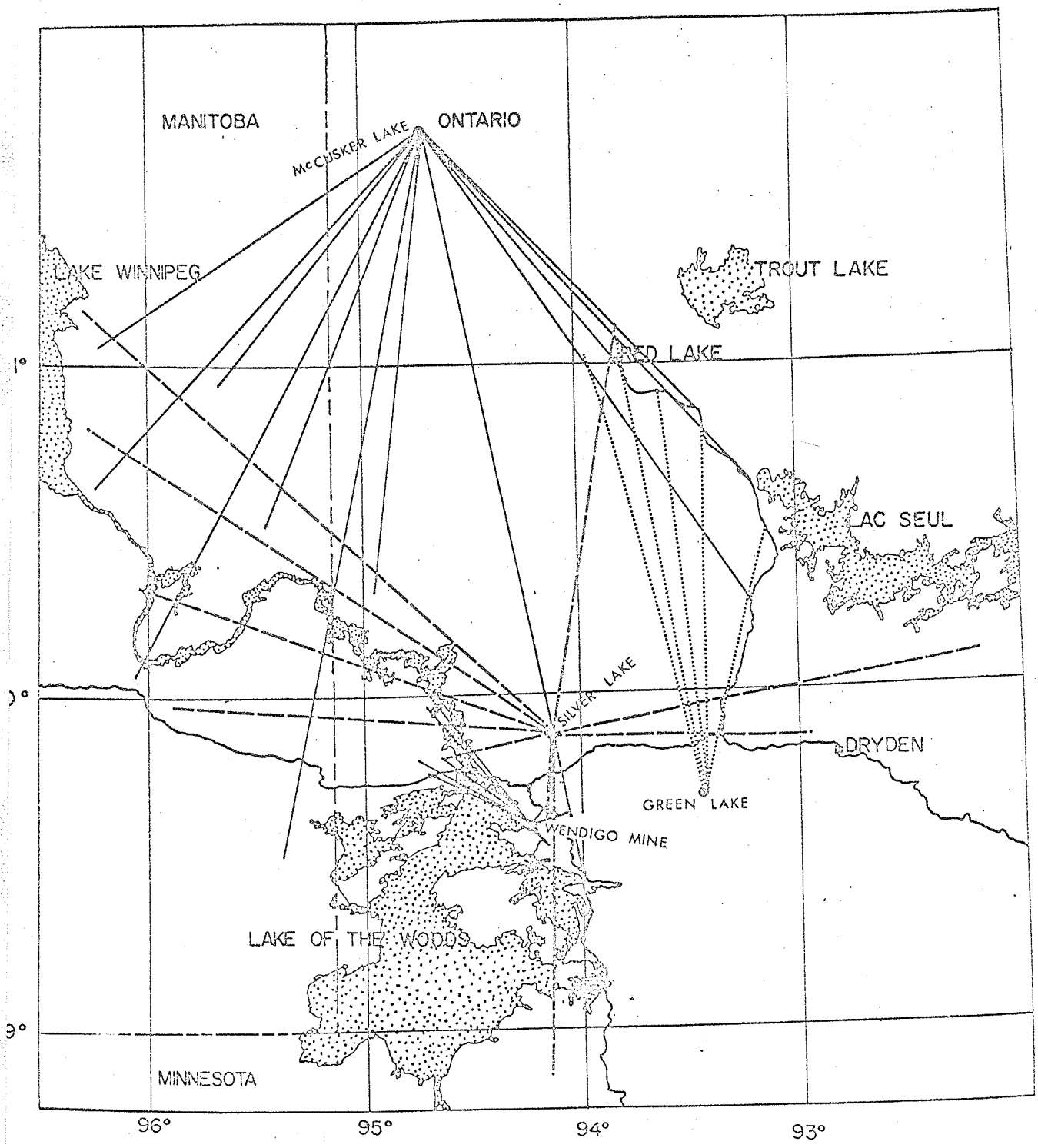

FIGURE 2. SHOT AND RECORDING LOCATIONS
(Lines join four shot points to various recording sites.
After Hall and Hajnal, 1968)

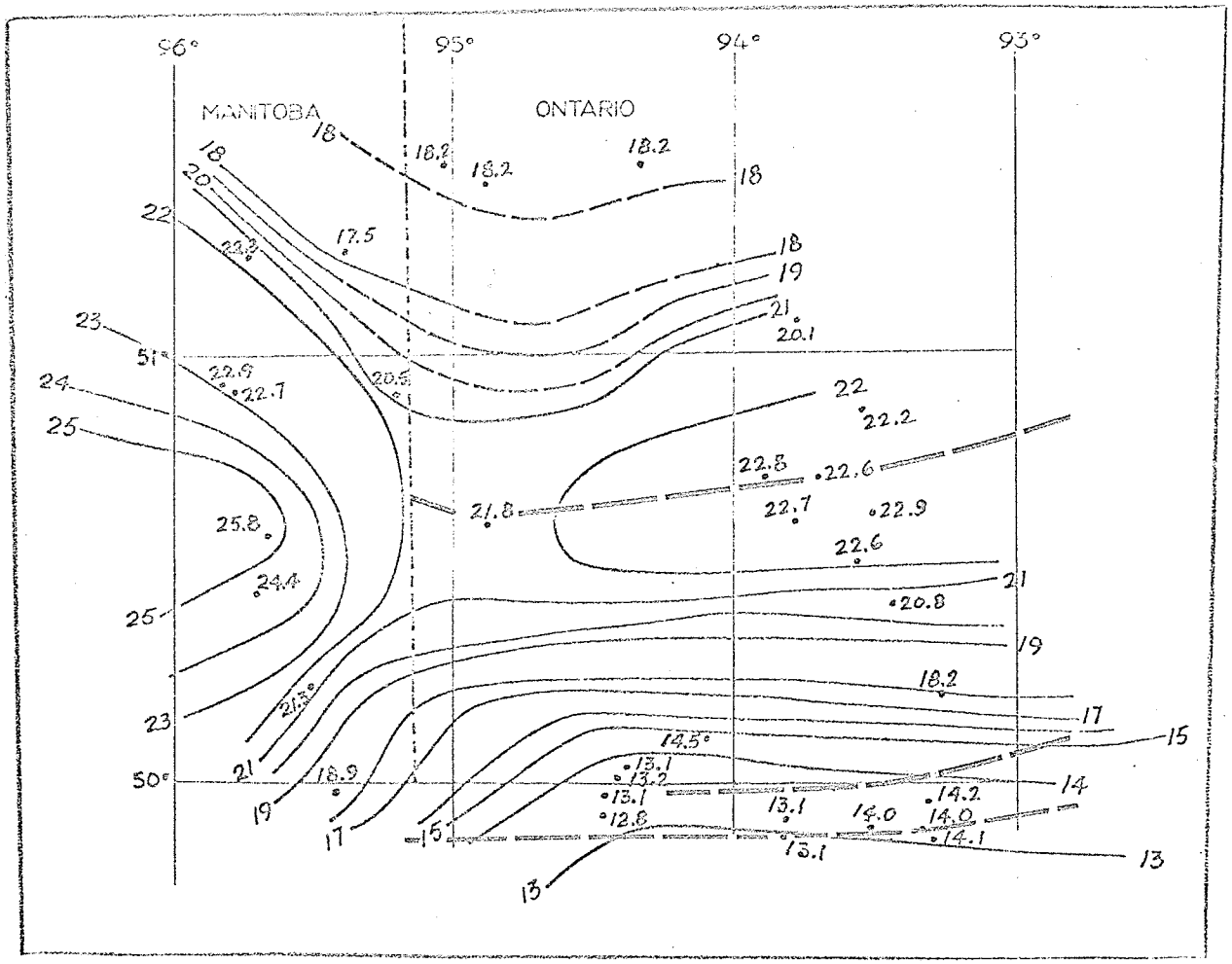

FIGURE 3. INTERMEDIATE DISCONTINUITY
(Kilometers. After Hall and Hajnal, 1968)

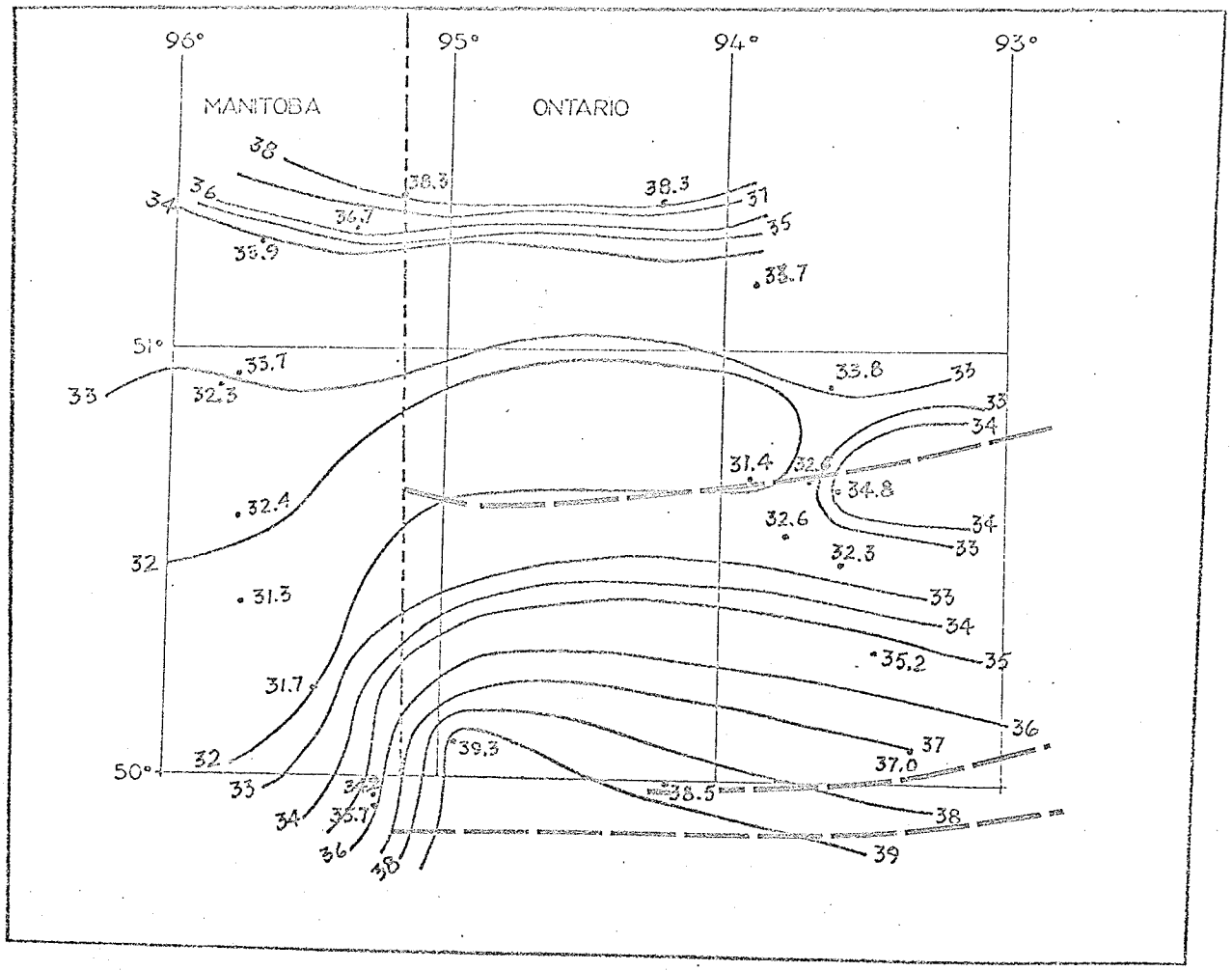

Gneissic Belt Boundaries

FIGURE 4. MOHOROVICIC DISCONTINUITY
(Kilometers. After Hall and Hajnal, 1968)

As can be seen in Figures 3 and 4, the Mohorovicic discontinuity comes to a high and the Intermediate to a low along a well-defined east-west trending belt which strikes parallel to the English River gneissic belt, but which is offset slightly northward from it.

The observed depths to the two surfaces shown in Figures 3 and 4 were smoothly contoured to produce the contour maps. It would be possible, however, to adjust contours between control points and produce maps of the two surfaces with narrow zones of rapidly changing depths. Thus the possibility of a block-like structure is raised.

The longitudinal or compressional wave velocities observed in the upper or granitic crustal layer, in the lower or basaltic layer and in the upper mantle are respectively $6.05 \pm .05$ km./sec., $6.85 \pm .05$ km./sec. and $7.92 \pm .05$ km./sec. (Hall and Hajnal, 1968).

Gravity Observations

At least two gravity surveys covering this area have been made. Innes (1960) has published a gravity map for north-western Ontario and Manitoba, and Brisbin and Wilson (1968) have done a more detailed survey into which Innes's values are incorporated. The two maps are in excellent accord with each other, except for some local anomalies of small extent which the more detailed survey detected and the other missed.

The gravity map of Innes (1960) from which Figure 7 is reproduced, shows a belt of high Bouguer anomalies directly over the gneissic belt and generally low Bouguer values over the complex belts of greenstone and granite plutons to the north and south.

Density Determinations

Innes (1960) has determined densities for many rock samples taken from locations in northern Ontario and eastern Manitoba. He lists six samples from locations which lie within the gneissic belt, along Ontario highway 105. Densities for these samples vary from 2.61 gm./cm.^{3} to 2.72 gm./cm.^{3}, and average 2.66 gm./cm.^{3}. For eighteen samples which were taken from the neighbouring complex belts both to the north and south, densities range from 2.60 gm./cm.^{3} to 3.10 gm./cm.^{3}, averaging 2.77 gm./cm.^{3}. The higher values represent greenstone and mafic schists; the lower values granitic rocks and sediments.

Brisbin and Wilson (1968) also find widely varying densities of samples, depending mainly on rock-types sampled. Averages of large numbers of samples show a somewhat lower average surface density for the gneissic belt than for the complex belts, in agreement with Innes (1960).

CHAPTER III

ISOSTASY, GRAVITY AND THE SEISMIC MODEL

Isostasy

The word isostasy comes from the Greek and means "equal standing" or "equal pressure" (Bowie, 1927). It describes an ideal condition of the outer portion of the Earth, including the crust and the rigid, upper-most mantle, together called the rigid crust (Heiskanen and Vening Meinesz, 1958, Ch. 2), whereby this outer material exerts a uniform pressure upon a layer below which behaves plastically for long-term stresses. This plastic layer or zone of weakness has been termed the asthenosphere from the Greek asthenes: weak, and is thought to coincide with the seismologists' waveguide (Beloussov, 1966). Woollard (1959) reports that from gravity and seismic data, the crust does in fact appear to float on denser mantle rock and that isostasy is approximated everywhere at some depth beneath the crust.

Early geodesists spent much time debating the relative merits of the Airy and Pratt concepts of isostasy. Such eminent geodesists as Hayford and Bowie supported Pratt's view of a uniform depth below sea level for the rigid crust, with topography compensated by decreased density beneath elevated areas. Airy's view, supported notably by Wegener and Heiskanen, held that the rigid crust has a uniform density but varies in depth, extending deeper, or forming a root under mountains, and rising to a shallow level under oceans. Subsequent geophysical

observations have verified the existence of mountain roots but horizontal density variation is also observed commonly. The two opposing views of Pratt and Airy constitute extreme positions: the real case lies somewhere between them.

The idea of a unique depth of compensation is a part of Pratt's theory. But it can be put together with the Airy theory as well. In this case, the depth of compensation for a particular region would be the lowest depth reached by a part of the rigid crust as it "floats" in the viscous layer. Under isostasy this would be the level of equal pressure for that region.

Both these theories of isostasy tacitly assume that when isostasy is achieved, all topographic features, regardless of extent, will be compensated by the mass distribution directly below. In this case, compensation is said to be "local" (Heiskanen and Vening Meinesz, 1958, Ch. 5). However such an assumption implies that the pressure at a point on the surface of compensation is hydrostatic, that is, due solely to the column of mass above it of arbitrary cross-section. It is known, however, that rock columns of smaller cross-section can be supported by adjacent rock columns, so that the force exerted on the surface of the Earth by a load covering a certain area, can be spread over a much larger area at the base of the rigid crust. The Vening Meinesz regional isostatic system (Heiskanen and Vening Meinesz, 1958, Ch. 5) provides for non-local compensation of small topographic masses. He assumes the crust to behave like an elastic plate which bends downwards into a viscous liquid when loaded, being strong enough to resist shear.

Conceivably, isostatic equilibrium could also be attained in discrete blocks. Within each block columns of mass would be supported by adjacent columns, but a whole block would act as a unit moving up or down in response to high or low pressure.

The concept of isostatic compensation has been widely applied to the study of post-glacial rebound wherein regions of the crust are believed to have been depressed to compensate for ice masses loading upon the surface.

If the isostatic adjustment by subsidence of a crustal load is not complete, and if there is a higher pressure at the base of the rigid crust than would prevail isostatically, there is said to be undercompensation. Conversely, if there is a lower than isostatic pressure at the base of the rigid crust, there is said to be overcompensation as would exist in a depressed region of the crust after melting of the ice load.

It should be clear that a crustal load need not be a mass upon the surface such as a mountain or an ice mass, but could lie anywhere within the crustal section as an anomalous mass or as relief on an interface between two layers of different densities. This is the case in the present study where surface topography is negligible.

Isostasy and the Initial Seismic Model

The contouring of observed depths to the Intermediate and Mohorovicic discontinuities as reproduced in Figures 3 and 4 depicts a two-layer crust whose interfaces are continuous. The Intermediate is at an average depth of about 20 km. and the Mohorovicic at an average depth

of about 35 km. Relief on the two surfaces is of the order of 5 km. maximum departure from the average depths.

The densities within the two crustal layers and upper mantle cannot be ascertained from the observed compressional wave velocities, but approximate values can be estimated. Based on empirical formulae, the densities are roughly 2.75, 3.00 and 3.30 gm./cm.^{3}, plus or minus about .05 gm./cm.^{3}.

Because of the fairly low density of control points in some areas, interpolation of contour lines between points might have masked narrow zones of rapidly changing interface depths. Even as it is, it can be seen, especially in the northern part of the map, but to the south also, that there are fairly narrow such zones.

For this model, the structural contour maps, Figures 3 and 4, were used to pick depths to Mohorovicic and Intermediate at eighty-five points evenly spaced at intervals of 10' latitude and 20' longitude. For these eighty-five pairs of depth values, the Intermediate depths d_1 were plotted as ordinates against the corresponding Mohorovicic depths d_2 as abscissae, as shown in Figure 5.

If the crust and uppermost mantle are in local isostatic equilibrium, then for any point on the surface, the depths d_1 and d_2 will be connected by the isostatic relation

$$\rho_1 d_1 + \rho_2 (d_2 - d_1) - \rho_3 (d_3 - d_2) = M \qquad (1)$$

where M is a constant, ρ_1, ρ_2, and ρ_3 are densities in the granitic layer, the basaltic layer and the upper mantle respectively, and d_3 is the depth of compensation in the upper mantle. From (1) it results immediately that

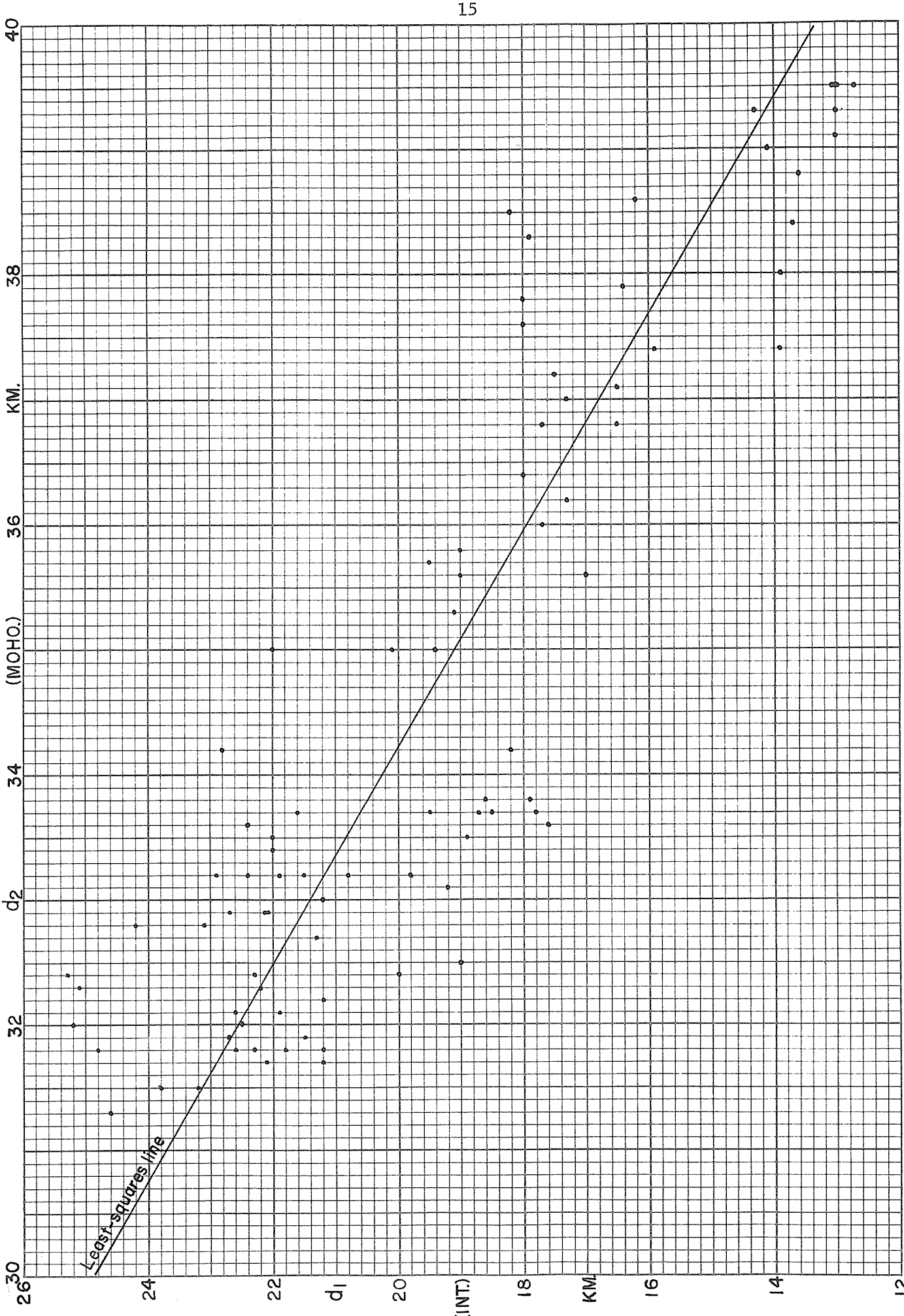

FIGURE 5. GRAPH OF INTERMEDIATE VS. MOHOROVICIC DEPTHS

$$d_1 = -\left[\frac{\rho_3 - \rho_2}{\rho_2 - \rho_1}\right] d_2 + C \qquad (2)$$

where C is a constant = $\dfrac{M - \rho_3 d_3}{\rho_1 - \rho_2}$

The following assumptions have been made in deriving this linear relation: that the elevation of the Earth's surface is essentially constant; that the densities ρ_1, ρ_2 and ρ_3 are uniform horizontally. The first is certainly valid and the second seems reasonable enough as a first approximation.

It is seen from Figure 5 that the points cluster about a straight line. The least-squares line is drawn through the eighty-five points. It has a slope of -1.15. If this agrees with the slope predicted from (2), it is excellent evidence in favour of nearly complete local isostasy. In order to evaluate this density-contrast ratio, a relation connecting ρ and V the longitudinal or compressional wave velocity is needed. It has been shown by several authors that a linear relation of the form

$$\rho = a + bV \qquad (3)$$

can be applied to a particular region as a good approximation for velocities over 6 km./sec. (Hall, 1968; Smith, Steinhart and Aldrich, 1966; Birch, 1961; Woollard, 1959).

From (3) then

$$\frac{\rho_3 - \rho_2}{\rho_2 - \rho_1} = \frac{V_3 - V_2}{V_2 - V_1} = 1.35 \pm .30 \qquad (4)$$

where V_1, V_2 and V_3 are the compressional wave velocities in the upper crustal, lower crustal, and uppermost mantle layers, respectively.

The negative slope of the least-squares line, 1.15, is well within the probable interval of 1.05 to 1.65. This agreement strongly indicates that local isostatic equilibrium very nearly prevails throughout this part of the crust.

Deviations from Isostasy

Although the points in Figure 5 cluster closely about a line which is taken to represent local isostasy, deviations from isostasy do occur, and they are represented by the scatter of points about the least-squares line. These deviations can be computed and mapped. They are directly related to pressure differences at the reference level.

For a particular Mohorovicic depth d_2, the corresponding least-squares value for the Intermediate depth shall be denoted $\overline{d_1}$. Then for a particular point (d_1, d_2) its "deviation from local isostasy" can be expressed quantitatively by $(d_1 - \overline{d_1})$. Positive values of $(d_1 - \overline{d_1})$ indicate areas of overcompensation which are isostatically light and negative values indicate areas of undercompensation which are isostatically heavy. These deviations have been mapped and contoured (Figure 6).

The English River gneissic belt appears to correlate with a belt of overcompensation which is deficient in mass or isostatically light. The overcompensation is greatest at the west extremity of the map area and is also high at the east extremity. There is a limited area of slight undercompensation within the gneissic belt at the southwestern corner of the mapped portion of the belt. The extreme southern portion

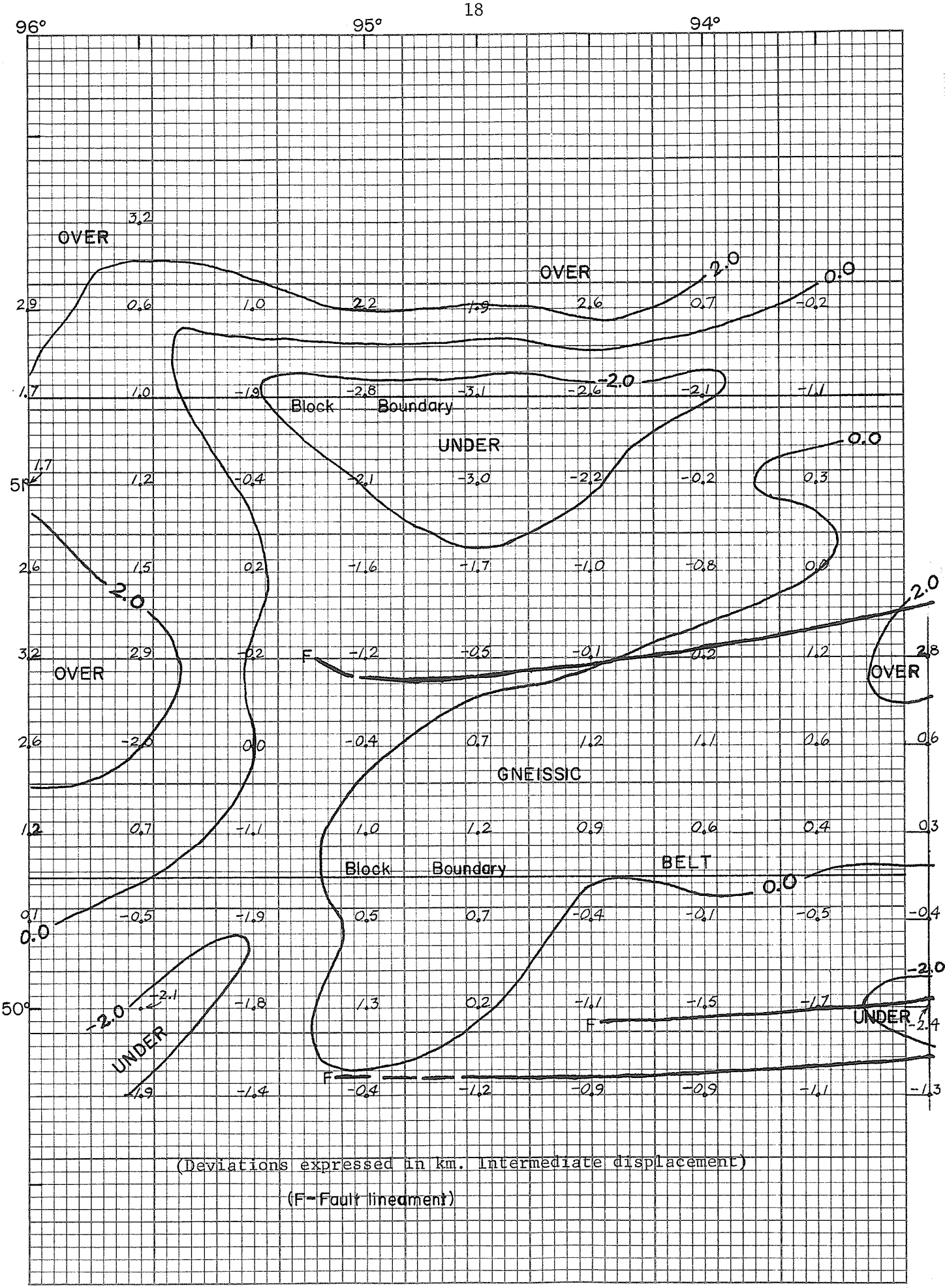

(Deviations expressed in km. Intermediate displacement)

(F-Fault lineament)

FIGURE 6. MAP OF DEVIATIONS FROM ISOSTASY

of the map shows overall undercompensation or a mass excess, and the northernmost portion is on the whole overcompensated or deficient in mass.

From Figure 7, reproduced from Innes (1960), it can be seen that the English River gneissic belt also correlates with a Bouguer gravity high. Figure 8 also shows, in profile, the gravity high and overcompensation over the gneissic belt. The correlation of the gneissic belt with an area of overcompensation and with a gravity high is inconsistent; that is, the two things are incompatible. An overcompensated area is isostatically light or deficient in mass. Such a deficiency would on a regional scale give rise to a Bouguer gravity low, and especially so if the upper crustal layer, of relatively low density, is anomalously thick under a good deal of the area.

The net overcompensation of the northern portion, however, does not present any great problem from the gravity standpoint because a Bouguer low is observed over this area. The quantitative agreement of the overcompensation and the gravity low will be determined by the comparison of theoretical and observed gravity profiles.

There appears to be more mass beneath the gneissic belt than the seismic model would indicate. If the seismic model is inadequate, then either the depths to interfaces are wrong, or the assumed density distribution is wrong. It is extremely unlikely that the depths calculated are in such error as to cause the disagreement. It is almost certain that the assumption of a horizontally uniform density distribution is incorrect.

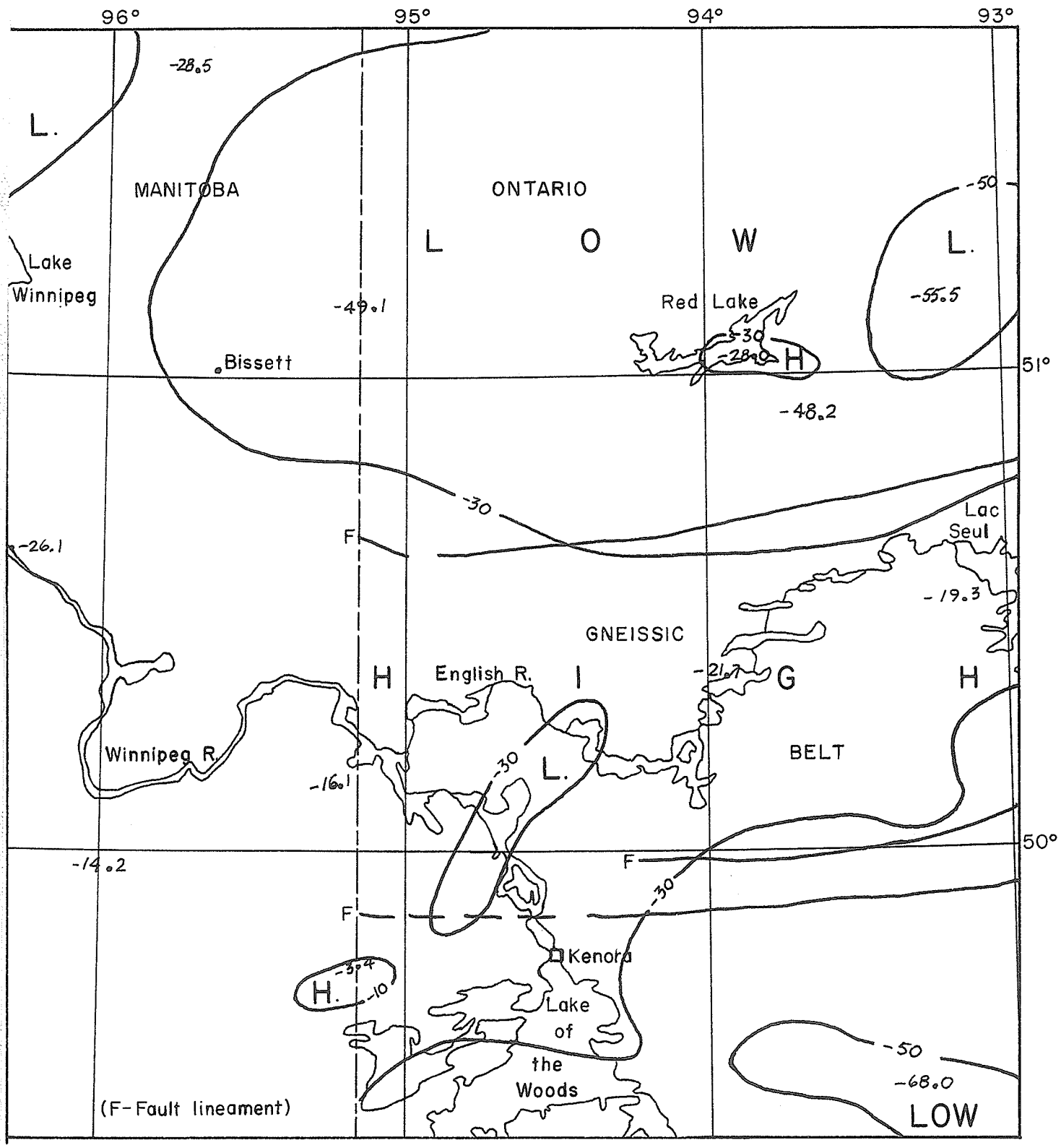

FIGURE 7. BOUGUER GRAVITY MAP

(Mgal. After Innes (1960))

Steinhart and Meyer (1961) report that their procedure in developing a crustal model is to start with a simple model then to look for departures from this starting-point. A model is first assumed to have planar interfaces and uniform velocity (or density) within layers. Departures from this simple model more commonly found are, they say, deviations of interfaces from planes and horizontal velocity (or density) variations, the latter especially in upper layers. So it would seem that such density variations could quite plausibly be suggested as the cause of the disagreement between gravity and degree of compensation according to the continuous crustal model.

To produce this gravity high then there must be a density anomaly somewhere beneath the gneissic belt. Surface samples reveal a somewhat lower surface density in the gneissic belt so the density anomaly must lie at some depth in the crust or upper mantle. However, if the structural feature in the crust is related to, and connects with the gneissic belt, and this seems reasonable, the density anomaly would have to be situated fairly near to the surface, at least at its highest extent. For if the anomalous mass were deeper it would also lie further northward and, therefore, the gravity effect would be offset northward and perhaps spread out over a wider area. The effects of different density anomalies of different distribution are briefly examined in the next chapter. It is shown that a rather small density anomaly in the upper crust beneath the gneissic belt can produce an appreciable gravity effect.

It is not unreasonable to imagine dense, very high-grade metamorphic rocks lying below the gneisses on the surface in the gneissic

belt which are themselves high-grade rocks. Such rocks would probably have higher seismic velocities than the rocks to the north or the south but this could easily have gone undetected due to their limited extent. It is quite possible also though that the velocities would not be significantly higher (Birch, 1961).

The Vertical Block Model

The contouring of depths to the two interfaces could have smoothed over rapid changes of depth in places. The values of the observed depths are distributed rather unevenly being fairly constant over three wide belts that trend east-west. This distribution suggests the possibility of a block-like structure, "blocks" being separated by vertical or subvertical boundaries, or perhaps by narrow zones of rapidly changing interface depths.

In Figure 8 a section is drawn showing observed depths and their north-south position. The positions of hypothetical vertical block boundaries have been set from this section and from the map of deviations from isostasy (Figure 6). On the section the places where depths change most rapidly roughly coincide with boundaries of the three belts of Figure 6. The vertical block boundaries are indicated in both Figures 6 and 8 at 50° 15' and 51° 10'.

The conception of this model is purely for purposes of making simplified gravity calculations. This vertical-block model provides a close approximation to the actual distribution of mass, it is felt, and is therefore used as a basis for computing the theoretical regional

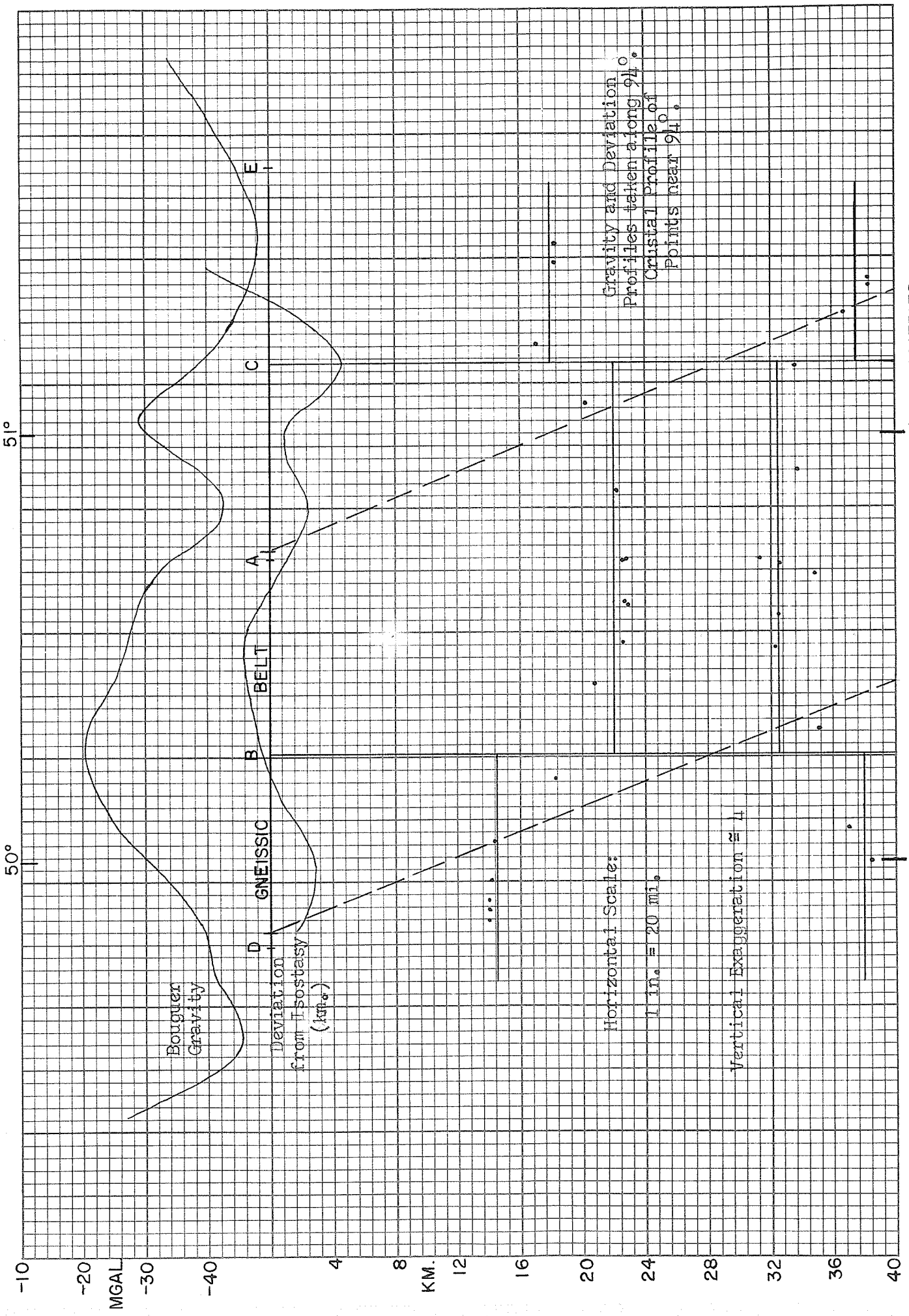

FIGURE 8. CRUSTAL SECTION WITH GRAVITY AND ISOSTATIC DEVIATION PROFILES

gravitational profile. Whether such a model is reasonable geologically is examined presently. Certainly, the existence of crustal blocks in the Basin and Range province of the western U.S.A. and in many grabens throughout the world is widely accepted.

In the gravity calculations the vertical blocks are considered to be horizontally layered. Representative values of seismic depths to the Intermediate and Mohorovicic discontinuities have been chosen as:

	Intermediate	Mohorovicic
South block	14.5 km.	38.0 km.
Central block	22.0 km.	32.5 km.
North block	18.0 km.	37.5 km.

The three blocks are considered to be two-dimensional, that is, of infinite extent in the east-west direction, and the central block is taken to be 100 km. wide (about 55' of latitude). The north and south blocks extend to infinity in three directions.

Over a point 50 km. distant from both the north and south boundaries of the central block, the gravitational acceleration is given by

$$g \cong C_o - 2\pi G b \sum_i \Delta V_i \left[d_i - \frac{2}{\pi w} \left(d_i^2 - \overline{d_i^2} \right) + \frac{4}{3\pi w^3} \left(d_i^4 - \overline{d_i^4} \right) \right] \qquad (5)$$

(Appendix A)

where C_o is a constant;

G is the universal gravitational constant;

d_i is the depth to the i th interface in the central block;

$\overline{d_i^2}$ and $\overline{d_i^4}$ are the averages of the squares and fourth powers of depths to the i th interface in the two adjacent blocks;

w is the width of the central block;

ΔV_i is the velocity contrast across the i th interface;

b is the constant in (3) representing the slope of the ρ vs. V curve.

Over the boundary of two blocks, for example, between the south and central blocks, the acceleration of gravity is given by

$$g \cong C_o - 2\pi G b \sum_i \Delta V_i \left[\overline{d_i} - \frac{1}{\pi w} \left(\frac{d_i^2 - D_i^2}{2} \right) + \frac{1}{6\pi w^3} \left(\frac{d_i^4 - D_i^4}{2} \right) \right] \qquad (6)$$

where $\overline{d_i}$ is the average of the depths to the i th interface in the south and central blocks;

d_i is measured in the central block;

D_i is measured in the north block.

Clearly "south" and "north" can be interchanged to give the gravitational acceleration over the boundary of the north and central blocks.

Over the south block, a distance $w/2$ or 50 km. from the central block

$$g = C_o - 2\pi G b \sum_i \Delta V_i \left[d_i - \frac{2}{\pi w} \left(\frac{d_i^2 - D_i^2}{2} \right) + \frac{4}{3\pi w^3} \left(\frac{d_i^4 - D_i^4}{2} \right) \right.$$

$$\left. - \frac{2}{3\pi w} \left(\frac{D_i^2 - \partial_i^2}{2} \right) + \frac{4}{81\pi w^3} \left(\frac{D_i^4 - \partial_i^4}{2} \right) \right] \qquad (7)$$

where d_i is measured in the south block;

D_i is measured in the central block;

∂_i is measured in the north block.

Once again interchanging "south" and "north" above will clearly give the corresponding gravitational acceleration over the north block.

Since C_o is generally unknown, gravity anomalies, rather than absolute gravitational accelerations, are calculated, and an arbitrary

constant is added to bring the theoretical and observed profiles to a common mean level. For the assumed block structure, assuming uniform densities in the upper crustal, lower crustal and upper mantle layers, and using (5), (6) and (7) theoretical Bouguer anomalies from south to north (Figure 5) are:

$$g_D = -20 \text{ mgal.}$$

$$g_B = -29 \text{ mgal.}$$

$$g_A = -37 \text{ mgal.}$$

$$g_C = -41 \text{ mgal.}$$

$$g_E = -43 \text{ mgal.}$$

These values have been plotted in Figure 9 for comparison with the observed Bouguer gravity profiles along 94° and 95° longitude. The agreement is quite good for the three northernmost points A, C and E but g_B is too low by some 7 mgal. and g_D is too high by about 12 mgal.

It was stated previously that a density anomaly beneath the gneissic belt is very strongly indicated. Such an anomaly has not been considered in calculating these gravity values. The effect of possible density anomalies which could improve the agreement of the theoretical and observed gravity profiles is considered in the next chapter. Also, the surrounding crust from which there is little or no seismic data does, of course, contribute to the gravity values, especially to g_D and g_E. The effects of reasonable models for these parts of the crust upon the theoretical gravity is also considered.

The Parallelepiped Model

Although the vertical block model is consistent with the seismic

data and within reason from gravity considerations, it appears less reasonable from a physical or geological point of view. It seems unlikely that a distinct surface feature like the gneissic belt, roughly the same width as the structural feature in the crust below, and trending parallel to it for at least 200 km., is not, in fact, the surface expression of the crustal structure below. The gneissic belt would then be the top surface of a block with sides dipping at about 45^{o}, that is, a parallelepiped of infinite horizontal extent in the direction of strike of the sides. The geological evidence, indicative of faults bounding the belt which could then be identified with the dipping sides of the block, would then support the physical as well as the mathematical existence of blocks or parallelepipeds.

A parallelepiped with sides dipping at 45^{o} (Figure 8) would join up the gneissic belt with the crustal structural features. The deepest part of the Intermediate discontinuity is in fact offset slightly southwards from the shallowest part of the Mohorovicic discontinuity. Changing the boundaries of the block model from vertical to 45^{o} dipping does not change significantly the position of the anomaly-causing masses in the Intermediate downwarp or in the Mohorovicic upwarp. So no significant change in the theoretical gravity anomalies will result from altering the crustal model in this way.

CHAPTER IV

DEDUCTIONS AND CONCLUSIONS

Improvement of the Crustal Model

It was stated previously that if more mass is given to the upper crust of the central block of the parallelepiped model, the theoretical gravity profile will agree better with the observed gravity, and the overcompensation, which was apparent in the original continuous model, would be greatly reduced, meaning that isostatic compensation would be more complete than the original model suggested. The effects of two possible distributions are considered: first, a density anomaly in a rectangular slab 90 km. wide in the top 5 km. of the crust under the gneissic belt; second, a density anomaly in the entire upper crust of the central parallelepiped, extending to 22 km. depth.

It is not suggested that either of these volumes actually exists as a distinct body within the crust. It is known for instance that neither of these volumes could actually extend to the surface where density sampling shows lower average densities within the gneissic belt. However, denser rocks could exist, say, 50 m. below the surface, or, the dense volcanic rocks in the areas north and south of the gneissic belt may be just thin ribbons, below which lighter rocks, presumably the extensions to depth of the granitic plutons, contrast with the slightly denser metamorphic rocks in the central block. In any case, the purpose of the calculations is to determine in general terms whether

the density anomaly indicated could be deep or shallow in the central block or parallelepiped, and to determine its order of magnitude.

The slab of 5 km. depth (Appendix B) has its northern edge at A and its southern edge 10 km. north of D. For calculations at D the effect of a slab 10 km. wide is subtracted from the effect of one 100 km. wide. At B the slab can be considered to be either 90 or 100 km. wide; the difference is insignificant.

At A, using a relation analogous to (6), the anomalous gravitational acceleration Δg_A due to the slab is given by

$$\Delta g_A = -\pi G \Delta\rho \left[d - \frac{d^2}{\pi w} + \frac{d^4}{6\pi w^3} \right] \tag{9}$$

from which $\Delta g_A = 103/|\Delta\rho|$ mgal. (10)

(Note that $\Delta\rho$, the density contrast at the depth d, is here negative with a higher density above than below.)

For Δg_B the anomaly is given, analogously to (5) by

$$\Delta g_B = -2\pi G \Delta\rho \left[d - \frac{2d^2}{\pi w} + \frac{4d^4}{3\pi w^3} \right] \tag{11}$$

from which $\Delta g_B = 202/|\Delta\rho|$ mgal. (12)

For Δg_D the additional anomaly is given by

$$\Delta g_D = \Delta g_A - \pi G \Delta\rho \left[d - \frac{d^2}{\pi w'} + \frac{d^4}{6\pi w'^3} \right] \tag{13}$$

from which $g_D = 14/|\Delta\rho|$ mgal. (14)

In the above d is the vertical thickness of the slab, w its width, w' the distance between D and the south edge of the slab, and $\Delta\rho$ the density contrast in gm./cm.^{3}.

The best fit with observed gravity is obtained when a density anomaly of .07 gm./cm.^{3} is chosen, and its effect is combined with the gravitational effects of reasonable crustal models north and south of the study area. Such "reasonable" models are specified later in this section. As is seen in Figure 9, the agreement is excellent.

The effects of a density anomaly in a parallelepiped extending to 22 km. depth, the Intermediate discontinuity in the central block, is now considered. A relation for calculating anomalies due to such a body is given by Grant and West (1965, Ch. 10), and is adapted to this particular case in Appendix B. From it the additional anomalies are

$$\Delta g_D' = 100.5\ /\Delta\rho/\ \text{mgal.}$$

$$\Delta g_B' = 764.1\ /\Delta\rho/\ \text{mgal.}$$

$$\Delta g_A' = 753.0\ /\Delta\rho/\ \text{mgal.}$$

$$\Delta g_C' = 88.7\ /\Delta\rho/\ \text{mgal.}$$

$$\Delta g_E' = 23.9\ /\Delta\rho/\ \text{mgal.}$$

Using a density anomaly of .015 gm./cm.^{3} gives the best agreement from these values. The agreement is not as good as for the case where the anomalous mass is nearer to the surface; however, the deviation of this theoretical profile from the observed is not sufficient to rule out this possibility. The effect of this distribution for $/\Delta\rho/$ = .015 gm./cm.^{3}, together with the effects of reasonable hypothetical blocks to the north and south, is also shown in Figure 9. Somewhat better agreement is obtained by supposing the extra mass or density anomaly to lie near the top of the upper crustal layer.

On the gravity map (Figure 7) it is seen that to the south and southeast of the area of study there is a widespread region of quite low Bouguer anomalies. This is, in effect, pulling down the south end of the observed gravity profiles in Figure 9. The effect of this part of the crust can be corrected for somewhat by including in the theoretical gravity calculations the effect of a hypothetical crustal block lying south of the south block. As a rough approximation, the south block is assumed to be 100 km. wide and a hypothetical block, which may be called the Rainy River block, is supposed to extend from the south block to infinity. Values of 14.5 km. and 41.0 km. as depths to the Intermediate and Mohorovicic have been chosen as being reasonable. There is in fact an observed Intermediate depth of 14.8 km. at the southeast corner of Lake of the Woods (Figure 3). Also, according to Goodwin's (1968) map of crustal thickness in North America, the 40 km. contour passes right through Lake of the Woods, and from there, the Mohorovicic drops to the south and east to 50 km. around the shore of Lake Superior. So such a hypothetical block is not at all unreasonable as a correction to the model. It is simply stated here that the effect of the Rainy River block would be to add to the gravity profile at D, B and A

$$\Delta g_D'' = -9 \text{ mgal.}$$

$$\Delta g_B'' = -4 \text{ mgal.}$$

$$\Delta g_A'' = -1 \text{ mgal.}$$

It can also be seen that to the north of the north block, Bouguer anomaly values rise somewhat from their low over the north block. Presumably, the gravitational attraction of the crust there is greater and tends to raise the north end of the gravity profiles (Figure 9). Accordingly a hypothetical North Patricia block is postulated, with depths to Intermediate and Mohorovicic of 15.0 km. and 37.5 km. respectively. Similarly, the north block is assumed to be 100 km. wide and the North Patricia block to go to infinity northward. The gravity effect of such a block at C and E is

$\Delta g_C'' = 1$ mgal.

$\Delta g_E'' = 3$ mgal.

These corrections are included with the change due to density anomalies in Figure 9. Whether the Bouguer low over the Rainy River area or the Bouguer high over the North Patricia area (relative to the low over the north block) is due to the hypothetical block postulated in each case is not important. It is in fact true, however, that something is causing these anomalies; and, therefore, quantitative estimates of the effects of these causes upon the actual gravity profiles have been made for reasonable assumed causes.

Employing (10) and (12) for $/\Delta\rho/ = .07$ gm./cm.^{3}, and (17) and (18), the theoretical gravity anomalies from an improved model, which assumes an anomalous mass to exist in the top 5 km. below the gneissic belt, are

$g_D = -31$ mgal.

$g_B = -22$ mgal.

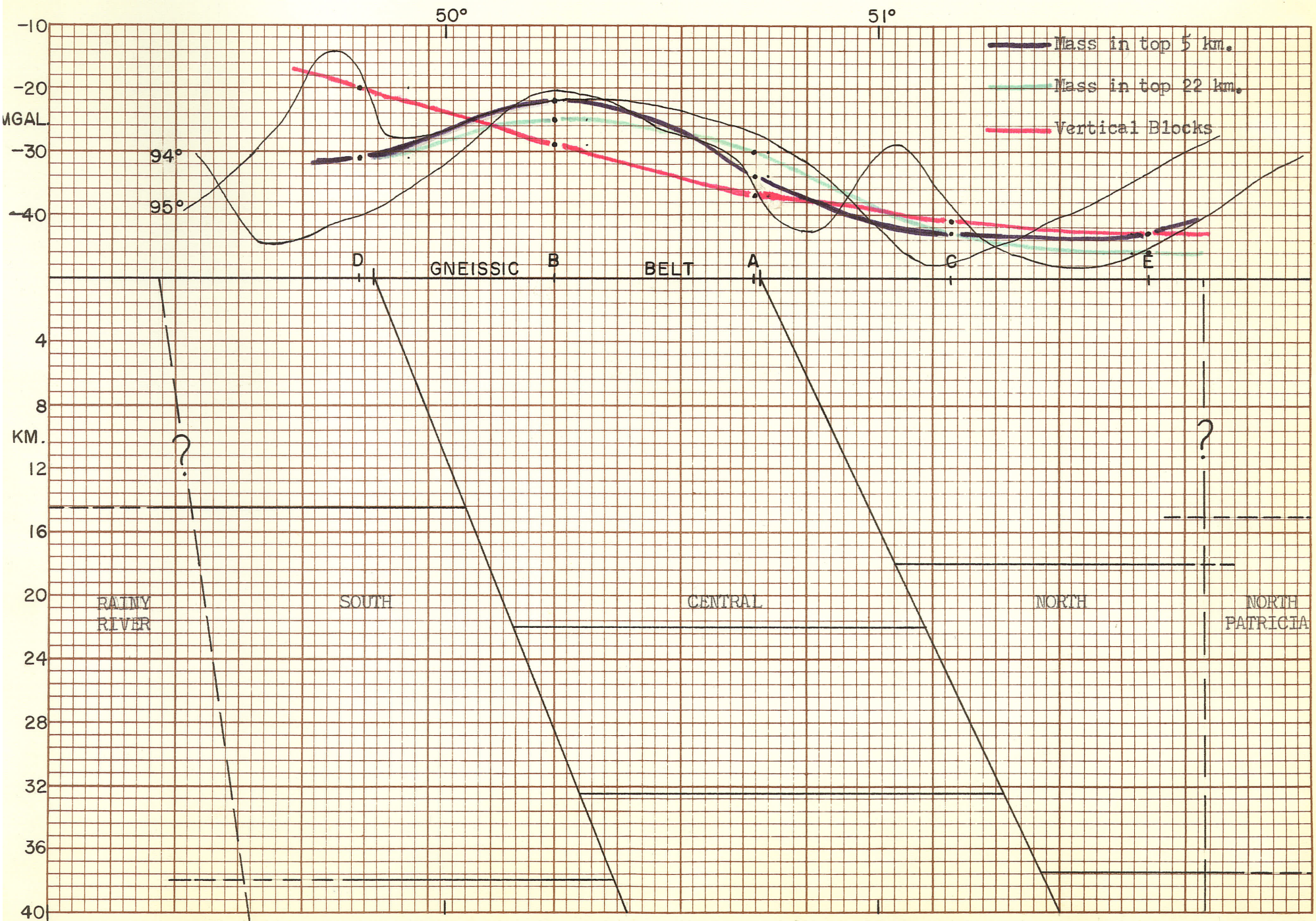

FIGURE 9. THEORETICAL AND OBSERVED GRAVITY PROFILES

g_A = -34 mgal.

g_C = -43 mgal.

g_E = -43 mgal.

The theoretical values assuming an anomalous mass to be spread throughout the top 22 km. are

g_D = -31 mgal.

g_B = -25 mgal.

g_A = -30 mgal.

g_C = -43 mgal.

g_E = -46 mgal.

Vashchilov and Markunskiy (1966) develop a method for extending seismic mapping horizontally by use of gravity maps, based on a stratified sub-vertical block structure of the crust and upper mantle. In a much cruder fashion this is what has been done here, though theoretical anomalies over the centers of the Rainy River and North Patricia blocks themselves were not actually calculated for comparison. A rigorous computation to extend the seismic data in northwestern Ontario by gravity maps, and later comparison with subsequent seismic data, might be considered for future work.

Processes in the Origin of the Gneissic Belt

It would be impossible to decide here upon one origin or another for the surface expression and deep structure of the crust in this area of northwestern Ontario. This remains a matter of conjecture until much more geological information is available, and to

consider this aspect extensively is not within the scope of this study. A brief consideration of the problem is given.

The evidence of faults bounding the belt as well as the high-grade rocks at the surface within the gneissic belt suggest the possibility that this central block has been uplifted (Wilson and Brisbin, 1968). Gneisses are typically formed at depths of some 5 to 10 km., or deeper, by regional metamorphic processes, probably in association with igneous intrusions (Huang, 1962, Ch. 9). Identification of paragneisses and metagreywackes, as yet uncertain, in the gneissic belt would suggest a geosynclinal environment of sedimentation. This would be consistent with the theory of continental growth from proto-continents, growing by the addition of orogenic belts on their margins, in the case of the gneissic belt, on the margin of the Superior protocontinent (Goodwin, 1968; Wilson, 1949). The narrowness of this belt in comparison with more recent geosynclines is consistent with the thinness of the Archaean crust (Gill, 1948).

The validity of connecting the gneissic belt with the warped or discontinuous crustal interfaces below, by deep faults dipping at 45^{o}, could be questioned. However, the Mohorovicic structure is off-set slightly northward from the Intermediate, which supports this idea. There is also some evidence that the angle of dip of a gravity fault plane, which would be roughly 60^{o} under surface conditions, will be less, that is, closer to 45^{o}, under conditions of high temperature and confining pressure, at least for some rock types (Badgley, 1965, Ch. 2; Handin and Hager, 1957, 1958).

The explanation of a high in the Mohorovicic and a low in the Intermediate on the geosynclinal hypothesis could be that this structure reflects the thin original crust at a continent-ocean margin.

Another cause of the crustal structure could have been processes in the mantle which worked upwards into the crust. Such processes could have given rise to regional metamorphism. The influence of mantle processes upon the crust is discussed by Beloussov (1966) and Subbotin (1965), for example. Vashchilov and Markunskiy (1966) state that magmatic and metamorphic processes and tectonic disturbances can cause the formation of blocks with subvertical boundaries, having horizontal dimensions of a few tens to a thousand kilometers. The subvertical borders of such blocks, they conclude, are deep fractures.

The possible effects of horizontal stress in the crust are examined by Ramberg and Stephansson (1964), Heiskanen and Vening Meinesz (1958, Ch. 10), Biot (1961) among others. It would appear that horizontal tension could produce parallel gravity faults, as well as diverging faults forming a graben. Compression would probably give rise to low angle thrust faults, which do not seem likely in the English River area from the cyclic occurrence of belts of alternating rock types and from the structural evidence.

Pressure Differences

It was stated earlier that the degree of isostatic compensation

is directly related to pressure at the reference level. Equation (1) expresses complete isostatic compensation, with M constant. Actually, M is the pressure which would exist hydrostatically at the reference level d_3, beneath some point on the surface. This expression can be rewritten

$$M = d_3 \rho_3 - d_2 (\rho_3 - \rho_2) - d_1 (\rho_2 - \rho_1) \qquad (20)$$

This gives the excess pressure over that which would exist under isostasy. Figure 6 is a map of $(d_1 - \overline{d_1})$ for the continuous crustal model. A scale factor of $(-b \Delta V_1)$ (See Equation 3) will make pressure contours from the deviation contours. If each column of rock of arbitrary cross-section exerted its hydrostatic pressure at the reference level, these would be true pressure anomalies, within the limits of accuracy of the depths and densities. However, rock columns are supported by adjacent columns to an extent and, averaged over blocks, smaller pressure differences are seen. Using Smith, Steinhart and Aldrich's (1966) value for b of .27, the maximum pressure difference from Figure 7 is about .14 kbar. For the block model, the pressure difference between the south and north blocks is about .07 kbar. The pressure of the central block is intermediate, being about .025 kbar less than that of the south block. It is interesting to note that a hypothetical density anomaly of .07 gm./cm.^{3} in the top 5 km. across 90 km. of the central block will provide .03 kbar pressure to bring it into virtual isostatic equilibrium with the south block. An anomaly

of .015 gm./cm.^{3} through the top 22 km. will also provide .03 kbar and bring the two blocks just as close to isostasy.

Hall (1968) reports from seismic data that the English River area crust as a whole is quite near to isostatic equilibrium with western Hudson Bay and parts of the Canadian Arctic, is slightly lighter than Northern Manitoba, and slightly heavier than the Lake Superior crust taken as a whole.

The pressure differences which are observed in stable areas like the Shield give an idea of what sort of pressure differences can be withstood by the crust, both within a region like English River, and among different widely separated regions. The pressure difference of .07 kbar which is interpreted as existing between the north and south blocks would, if the crust were free to adjust and assuming it to float in a viscous layer of density 4.0 gm./cm.^{3}, give rise to an uplift of 175 m. This might be looked upon as a rough figure for that sort of anisostasy that can remain in narrow crustal blocks, although it is possible that some post glacial rebound has still to take place. Over 100 km. distance, this should not amount to much more than 10 m. or so if Andrews' (1968) figure of 100 m. residual uplift for a part of Hudson Bay is reasonable.

Conclusions

1. The crustal model developed from the geophysical data is one of a crust very nearly in complete local isostatic equilibrium.

2. The major departures from isostatic equilibrium in the initial seismic model may be explained by a density anomaly beneath the gneissic belt which also accounts for a belt of Bouguer gravity high over the gneissic belt.

3. The anomalous mass would appear to be in the upper crustal layer if the gneissic belt and crustal structure are really connected to form a parallelepiped block.

4. Such an anomalous mass would bring the south and central blocks very close to isostatic equilibrium, but the north block appears somewhat isostatically light, or overcompensated.

5. A density anomaly of a few hundredths of a gm./cm.^{3} in the top 5 or 10 km. of the crust would account for the gravity anomaly over the gneissic belt.

APPENDIX A

THEORETICAL GRAVITY ANOMALIES DUE TO A STRATIFIED-BLOCK CRUSTAL MODEL

The analytical expression for the vertical gravitational acceleration due to a rectangular, two-dimensional body (extending to infinity in the third dimension) is given by Heiland (1963, Ch. 7). In the two-dimensional picture x is the horizontal coordinate, which is zero above one edge of the body, and equal to w over the other edge of the body, w being the width of the body. Then the gravitational acceleration, from Heiland's equation (7-42b) is

$$g = 2G\rho\left\{x \cdot \ln\sqrt{\frac{d_i^2 + x^2}{d_i^2 - 1 + x^2}} - (x - w)\cdot \ln\sqrt{\frac{d_i^2 + (x - w)^2}{d_{i-1}^2 + (x - w)^2}}\right.$$
$$\left. + d_i\left[\tan^{-1}\left(\frac{x}{d_i}\right) - \tan^{-1}\left(\frac{x - w}{d_i}\right)\right] - d_{i-1}\left[\tan^{-1}\left(\frac{x}{d_{i-1}}\right) - \tan^{-1}\left(\frac{x - w}{d_{i-1}}\right)\right]\right\} \quad \text{(A-1)}$$

where d_{i-1} is the depth to the upper surface of the body; d_i is the depth to the lower surface of the body; all other symbols have the same meaning as in Chapter III.

Over the center of such a rectangular prism, at $x = w/2$, (A-1) reduces to

$$g = 2G\rho\left\{\frac{w}{2} \cdot \ln\left[\frac{w^2 + 4d_i^2}{w^2 + 4d_{i-1}^2}\right] + 2d_i \tan^{-1}\left(\frac{w}{2d_i}\right) - 2d_{i-1} \tan^{-1}\left(\frac{w}{2d_{i-1}}\right)\right\} \quad \text{(A-2)}$$

The ln term in (A-2) can be approximated using

$$\ln(1 + y) = y - y^2/2 + y^3/3 - y^4/4 + \ldots \quad \text{(A-3)}$$

provided that

$$\frac{4\ (d_i^2 - d_{i-1}^2)}{w^2 + 4\ d_{i-1}^2} < 1 \qquad \text{(A-4)}$$

This condition is more than satisfied if

$$2d_i < w \qquad \text{(A-5)}$$

For values of d_2 not exceeding 41 km. and for values of w of about 100 km. considered in this study, this series (A-3) converges.

Use is also made of the relation

$$\frac{w\ d_i}{w^2 + 4\ d_i^2} = \frac{d_i}{w} - \frac{4 d_i^3}{w^3 + 4 w d_i^2} \qquad \text{(A-6)}$$

so that terms like the left-hand side of (A-6) can be split into a first-order term in d_i/w and a third-order term. The third-order term is quite small if

$$2\ d_i < w \qquad \text{(A-7)}$$

which is indeed the case.

The inverse tangent terms can be expanded in series using the relation $\tan^{-1}(1/z) = \pi/2 - \tan^{-1}(z)$ (A-8)

and then the expression

$$\tan^{-1}(z) = z - z^3/3 + z^5/5 - \ldots \qquad \text{(A-9)}$$

provided once again that

$$2\ d_i < w$$

Incorporating these series approximations (A-3) and (A-9), as well as (A-6) and (A-8), the expression (A-2) becomes

$$g = 2\pi G \rho \left[\Delta d_i - \frac{2}{\pi w} \Delta d_i^2 + \frac{4}{3\pi w^3} \Delta\ d_i^4 - \ldots \right] \qquad \text{(A-10)}$$

where $\Delta d_i = d_i - d_{i-1}$

$$\Delta d_i^2 = d_i^2 - d_{i-1}^2$$

$$\Delta d_i^4 = d_i^4 - d_{i-1}^4 \qquad \text{(A-11)}$$

If a rectangular prism or block of this sort is stratified in horizontal layers, the total gravitational acceleration is equal to the sum of the effects of the different layers. For the top layer $d_o = 0$, the density is ρ_1, and $d_1 - d_o$ is the thickness, and analogously for the i th layer, ρ_i is the density and Δd_i the thickness. Then

$$g = 2\pi G \sum_i \rho_i \left[\Delta d_i - \frac{2}{\pi w} \Delta d_i^2 + \frac{4}{3\pi w^3} \Delta d_i^4 - \cdots \right] \qquad \text{(A-12)}$$

Summing by parts, and assuming that

$$\rho_i = a + bV_i$$

(A-12) becomes

$$g = C - 2\pi G b \sum_i \Delta V_i \left[d_i - \frac{2}{\pi w} d_i^2 + \frac{4}{3\pi w^3} d_i^4 - \cdots \right] \qquad \text{(A-13)}$$

The first term in the brackets in (A-13), by itself, gives the gravitational acceleration for a block of infinite width. The second and third terms subtract the effect of two outer blocks each extending to infinity and bounding the central block of width w. If the effects of two such outer blocks is now included in g, the additional contribution is

$$C' - 2\pi G b \sum_i \Delta V_i \left[\frac{2}{\pi w} \overline{d_i^2} - \frac{4}{3\pi w^3} d_i^4 + \cdots \right] \qquad \text{(A-14)}$$

where $\overline{d_i^2}$ and $\overline{d_i^4}$ are the averages of d_i^2 and d_i^4 respectively in

the two outer blocks, which are in general different from one another and from the corresponding quantities for the central block. Adding (A-14) to g of (A-13) gives

$$g \cong C_o - 2\pi G b \sum_i \Delta V_i \left[d_i - \frac{2}{\pi w} \left(d_i^2 - \overline{d_i^2} \right) + \frac{4}{3\pi w^3} \left(d_i^4 - \overline{d_i^4} \right) \right]$$

which is the gravitational acceleration over the center of a central block flanked by two blocks which extend to infinity. The velocity contrasts over the various interfaces are assumed to be the same in all blocks. Actually only gravity anomalies are calculated from (A-15) because C_o (as well as C and C') are constants in general indeterminable.

Over the edge of a rectangular block or prism, that is at $x = o$ or $x = w$, (A-1) reduces to

$$g = 2G\rho \left\{ w/2 \ \ln \left[\frac{d_{i+1}^2 + w^2}{d_i^2 + w^2} \right] + d_{i+1} \tan^{-1} \frac{w}{d_{i+1}} - d_i \tan^{-1} \frac{w}{d_i} \right\} \quad \text{(A-16)}$$

Approximating the logarithmic and inverse tangent terms as was previously done and summing over several layers (A-16) becomes

$$g \cong C_o - 2\pi G b \sum_i \Delta V_i \left[d_i/2 - d_i^2/2\pi w + d_i^4/12\pi w^3 \right] \quad \text{(A-17)}$$

Over the boundary of two blocks of width w, g is the sum of two expressions like the right side of (A-17) so that

$$g \cong C_o' - 2\pi G b \sum_i \Delta V_i \left[d_i - \frac{1}{\pi w} \left(\overline{d_i^2} \right) + \frac{1}{6\pi w^3} \left(\overline{d_i^4} \right) \right] \quad \text{(A-18)}$$

To include the effect of the far flanking block, and the infinite extent of the near flanking block, a correction similar to (A-14) is included but $w/2$, the distance from the observation point to the flanking-block

boundary in the first case, now becomes w. The acceleration of gravity over the boundary of the central and near flanking block, with a far flanking block included is then

$$g \cong C_o - 2\pi G b \sum_i \Delta V_i \left[\overline{d_i} - \frac{1}{\pi w} \left(\frac{d_i^2 - D_i^2}{2} \right) + \frac{1}{6\pi w^3} \left(\frac{d_i^4 - D_i^4}{2} \right) \right] \tag{A-19}$$

where d_i is measured in the central block;

$\overline{d_i}$ is averaged in the two blocks adjacent to the observation point;

D_i is measured in the far flanking block.

Over one of the flanking blocks a distance $w/2$ from the central block boundary, the observation point can be considered to be over a central block adjacent to which are: on one side a block extending to infinity with the same d_i's;

on the other side a block, the actual central block, extending, in the first approximation, to infinity, but whose effect is corrected for the far flanking block which has its near boundary a distance $3w/2$ from the observation point, rather than $w/2$ as was the case in deriving (A-15).

First of all, ignoring the far flanking block g from (A-15) is given by

$$g \cong C'_o - 2\pi G b \sum_i \Delta V_i \left[d_i - \frac{2}{\pi w} \left(\frac{d_i^2 - D_i^2}{2} \right) + \frac{4}{3\pi w^3} \left(\frac{d_i^4 - D_i^4}{2} \right) \right] \tag{A-20}$$

where d_i is measured in the flanking block under the observation point and D_i is measured in the central block. From (A-14), the effect of

the far flanking block is to add

$$C' - 2\ Gb\sum_i \Delta V_i \left[-\frac{2}{3\pi w} \left(\frac{D_i^2 - \partial_i^2}{2}\right) + \frac{4}{81\pi w^3}\left(\frac{D_i^4 - \partial_i^4}{2}\right)\right] \tag{A-21}$$

to the value of g. Here, ∂_i is measured in the far flanking block. Then, over a flanking block a distance $W/2$ from the central block boundary

$$g \cong C_o - 2\pi Gb\sum_i \Delta V_i \left[d_i - \frac{2}{\pi w}\left(\frac{d_i^2 - D_i^2}{2}\right) + \left(\frac{4}{3\pi w^3}\right)\left(\frac{d_i^4 - D_i^4}{2}\right) - \frac{2}{3\pi w}\left(\frac{D_i^2 - \partial_i^2}{2}\right) + \frac{4}{81\pi w^3}\left(\frac{D_i^4 - \partial_i^4}{2}\right)\right] \tag{A-22}$$

APPENDIX B

GRAVITY ANOMALY
EXPRESSIONS FOR TWO DENSITY DISTRIBUTIONS

Rectangular Slab

The gravity anomaly due to a two-dimensional slab of depths 0 km. and 5 km. to upper and lower surfaces, and of width 90 km., can be calculated from (A-13) and corresponding relations considering the slab to be 100 km. wide with observation points over its center, edges, and points 50 km. and 100 km. beyond its north edge, and then correcting for a 10 km. slab at the south end. At the center or north edge the effect of this 10 km. portion is negligible. Over the center observation point

$$\Delta g = 2\pi G \Delta \rho \left[5.0 - .17 + .00027 - \ldots\right] \qquad \text{(B-1)}$$

Using values of depths in km., values of density in gm./cm.^{3} and G(= 6.668) in 10^{-8} c.g.s. units gives Δg in mgal., or 10^{-3} c.g.s. units.

So $\Delta g = 202/\Delta\rho/$ mgal. (B-2)

where $\Delta\rho$ is the density contrast over the interface at 5 km. depth which is negative when a positive density anomaly is assumed in the top 5 km.

Over the north edge of this slab the gravity anomaly, using (A-17), is

$$\Delta g = 2\pi G \Delta \rho \left[2.5 - .04 + .00002 - \ldots\right] \qquad \text{(B-3)}$$

$$\text{or } \Delta g = 103/\Delta\rho/ \text{ mgal.} \qquad \text{(B-4)}$$

At the observation point 10 km. south of the south edge the gravity anomaly is, from (A-17),

$$\Delta g = -2\pi G \Delta \rho \left[2.5 - 2.5 - .04 + .40 + .00002 - .017 + \ldots\right] \qquad \text{(B-5)}$$

$$\text{or } g = 14/\Delta\rho/ \text{ mgal.} \qquad \text{(B-6)}$$

At a point 50 km. north of the north edge, the gravity anomaly over the edge of a 50 km. slab is subtracted from the effect of a 140 km. slab using (A-17) whereby

$$\Delta g = -2\pi G\Delta\rho \left[2.5 - 2.5 - .03 + .08 + \ldots\right] \qquad \text{(B-7)}$$

$$\text{or } \Delta g = 2\ /\Delta\rho/ \text{ mgal.} \qquad \text{(B-8)}$$

For $/\Delta\rho/$ of less than .10 gm./cm.^{3} this produces a negligible gravity anomaly of about .2 mgal., negligible that is compared to the magnitudes of uncertainties in the model. Similarly, further north still the effect is even less.

Parallelepiped

The theoretical anomaly due to a parallelepiped, extending to infinity in the third dimension is given by Grant and West (1965, Ch. 10). Their equation (10-4), for depths of zero and 22 km. to upper and lower surfaces a width of 100 km., and dip of 45° to the north, becomes

$$\frac{\Delta g}{2G\delta} = \frac{x}{2}\left\{ \ln\left[\left(\frac{x-100}{x}\right) \cdot \sqrt{\frac{(x+22)^2 + 484}{(x-78)^2 - 484}} \right] + \tan^{-1}\left(\frac{x-22}{22}\right) - \tan^{-1}\left(\frac{x-78}{22}\right) + \tan^{-1}\left(\frac{x-100}{0}\right) - \tan^{-1}\left(\frac{x}{0}\right) \right\} +$$

$$50\left\{ \ln\left[\frac{\sqrt{(x-78)^2 + 484}}{(x-100)} \right] - \tan^{-1}\left(\frac{x-78}{22}\right) - \tan^{-1}\left(\frac{x-100}{0}\right) \right\} +$$

$$22\left\{ \tan^{-1}\left(\frac{x+22}{22}\right) - \tan^{-1}\left(\frac{x-78}{22}\right) \right\} \qquad \text{(B-9)}$$

In (B-9) x is the horizontal coordinate measured from the upper north edge of the parallelepiped, and is positive southward. Substitution of values of x of 110 km., 60 km., 10 km., -40 km. and -90 km. gives gravity anomalies from south to north at the same points as in the vertical block calculations. In (B-9) δ is the density excess in the parallelepiped block in gm./cm.^{3}.

LIST OF REFERENCES

Andrews, J. T. (1968). Postglacial rebound in Arctic Canada; similarity and prediction of uplift curves; Can. J. Earth Sci., 5, p. 39.

Badgley, P. C. (1965). Structural and Tectonic Principles; Harper and Row, Publishers, Inc., New York.

Beloussov, V. V. (1966). Modern concepts of the structure and development of the Earth's crust and the upper mantle of continents; Q. J. Geol. Soc. London, 122, p. 293.

Biot, M. A. (1961). Theory of folding of stratified viscoelastic media and its implication in tectonics and orogenesis; Bull. Geol. Soc. Am., 72, p. 1595.

Birch, F. (1961). Composition of the Earth's mantle; Geoph. J., 4, p. 295.

Bowie, W. (1927). Isostasy; E. P. Dutton and Co., New York.

Brisbin, W. C. and Wilson, H. D. B. (1968). Crustal structure of northwestern Ontario, III - Gravity; in press.

Clowes, R. M., Kanasewich, E. R. and Cumming, G. L. (1968). Deep crustal seismic reflections at near-vertical incidence; Geophysics, 33, p. 441.

Dwibedi, K. (1966). Petrology of the English River gneissic belt, northwestern Ontario and southeastern Manitoba; Ph. D. Thesis, University of Manitoba.

Gardner, L. W. (1939). An aerial plan of mapping subsurface structure by refraction shooting; Geophysics, 4, p. 247.

Gill, J. E. (1948). In reference in Wilson (1949); also, Mountain building in the Canadian Precambrian Shield; Int. Geol. Cong., Vol. of titles and abstracts, London, 1948.

Goodwin, A. M. (1968). Evolution of the Canadian Shield; Proc. Geol. Assoc. Can., 19, p. 1.

Grant, F. S. and West, G. F. (1965). Interpretation Theory In Applied Geophysics; McGraw-Hill Book Co., New York.

Hall, D. H. (1968). A seismic-isostatic analysis of crustal data from Hudson Bay; in press, Geol. Surv. Can.

Hall, D. H. and Hajnal, Z. (1968). Crustal structure of northwestern Ontario, II - Refraction seismology; in press.

Handin, J. and Hager, R. V., Jr. (1957). Experimental deformation of sedimentary rocks under confining pressure: Tests at room temperature on dry samples; Bull. Am. Assoc. Petrol. Geol., 41, p. 1.

Handin, J. and Hager, R. V., Jr. (1958). Experimental deformation of sedimentary rocks under confining pressure: Tests at high temperature; Bull. Am. Assoc. Petrol. Geol., 42, p. 2892.

Heiland, C. A. (1963). Geophysical Exploration; Hafner Publishing Co., New York.

Heiskanen, W. A. and Vening Meinesz, F. A. (1958) - The Earth and Its Gravity Field; McGraw-Hill Book Co., New York.

Huang, W. T. (1962). Petrology; McGraw-Hill Book Co., New York.

Innes, M. J. S. (1960). Gravity and isostasy in northern Ontario and Manitoba; Publ. Dom. Obs. Ottawa, 21, p. 263.

Parkinson, R. N. (1962). Operation overthrust; Roy. Soc. Can. Spec. Publ. No. 4: Tectonics of the Canadian Shield, p. 90.

Ramberg, H. and Stephansson, O. (1964). Compression of floating elastic and viscous plates effected by gravity, a basis for discussing crustal buckling; Tectonophysics, 1, p. 101.

Smith, T. J., Steinhart, J. S., and Aldrich, L. T. (1966). Lake Superior crustal structure; J. Geoph. Res., 71, p. 1141.

Steinhart, J. S. and Meyer, R. P. (1961). Explosion Studies of Continental Structure - University of Wisconsin, 1956 - 1959; Carnegie Inst. Wash. Publ. 622, Washington, D.C.

Subbotin, S. I., Naumchik, G. L., and Rakhimova, I. S. (1965). Structure of the Earth's crust and upper mantle; Processes in the upper mantle; Influence of upper mantle processes on the structure of the Earth's crust; Tectonophysics, 2, p. 111, 151, 185.

Vashchilov, Y. Y. and Markunskiy, V. S. (1966). Gravimetric studies of the stratified block structure of the Earth's crust; Izv. Acad. Sci., U.S.S.R., Phys. of the Solid Earth, 1966, p. 646.

Wilson, H. D. B. and Brisbin, W. C. (1968). Crustal structure of northwestern Ontario, I - Geology; in press.

Wilson, J. T. (1949). Some major structures of the Canadian Shield; Trans. Can. Inst. Min. Metal., 52, p. 231.

Woollard, G. P. (1959). Crustal structure from gravity and seismic measurements; J. Geoph. Res., 64, p. 1521.